The Canadian Mineralogist
Vol. 32, pp. 81-86 (1994)

THE VIBRATIONAL SPECTRA AND STRUCTURE OF NORDENSKIÖLDINE

DIEN LI

Department of Chemistry, University of Western Ontario, London, Ontario N6A 5B7

MINGSHENG PENG

Department of Geology, Zhongshan University, Guangzhou, Guangdong 510275, The People's Republic of China

G. MICHAEL BANCROFT

Department of Chemistry, University of Western Ontario, London, Ontario N6A 5B7

ABSTRACT

We report the infrared and Raman spectra of nordenskiöldine. Bands in the spectra of nordenskiöldine are assigned to the corresponding vibrational modes by a calculation of normal modes within the all-valence force-field model and by a comparison with calculated and measured results for the isostructural dolomite. The characteristic double peaks for the out-of-plane bending mode ν_2 and the asymmetric stretching mode ν_3 of the BO_3^{3-} group are attributed to the substitution effect of B^{11} and B^{10} in nordenskiöldine. The calculated intensities in the Raman spectra for nordenskiöldine and dolomite are related to the differences in electric dipole polarizabilities and to the electronic structure for BO_3^{3-} and CO_3^{2-} groups, consistent with the first-principles calculations.

Keywords: nordenskiöldine, dolomite, infrared-absorption spectra, raman spectra.

SOMMAIRE

Nous présentons les spectres d'absorption infra-rouge et de Raman de la nordenskiöldine. Les spectres sont identifiés par comparaison avec 1) avec les modes vibrationnels correspondants par calcul des modes normaux à l'intérieur du champ des forces fondé sur la totalité des valences, et 2) les résultats calculés et mesurés pour la dolomite, isostructurale. Les pics doubles caractéristiques qui décrivent le mode ν_2 de torsion hors du plan du groupe BO_3^{3-} et son mode ν_3 d'étirement sont attribués à l'effet de l'incorporation de B^{11} et B^{10} dans la structure. Les intensités calculées du spectre de Raman de la nordenskiöldine et de la dolomite résultent de différences dans la polarisabilité du dipole électrique et dans la structure électronique des groupes BO_3^{3-} et CO_3^{2-}, différences qui concordent avec les résultats de calculs à partir des principes de base.

(Traduit par la Rédaction)

Mots-clés: nordenskiöldine, dolomite, spectre d'absorption infra-rouge, spectre de Raman.

INTRODUCTION

The crystal chemistry of borate minerals is much more complex than that of carbonate minerals, which have isolated CO_3^{2-} groups only. The coordination polyhedra around the boron atoms in borate minerals are either triangles or tetrahedra, which can form polynuclear anions by polymerizing in various ways. The structural principles have been discussed by Christ (1960), Edwards & Ross (1960) and Wells (1984). In general, borate minerals can be divided into three classes: (1) those containing 3-coordinate boron only (*e.g.*, nordenskiöldine), (2) those containing 3- and 4-coordinate boron, such as borax, and (3) those containing 4-coordinate boron only, say sinhalite. On the other hand, even for the orthoborates and carbonates of the same crystal structure, apparent differences in spectral features are expected, mainly owing to the difference in the bonding and crystal-chemical properties (electronegativity, ionic radius) of boron and carbon.

Nordenskiöldine, a rare orthoborate mineral that contains discrete BO_3^{3-} groups, has been reported only in a few locations. It was discovered in an

alkaline pegmatite on the island of Arö, in the Langesund fiord, southern Norway, by Brögger in 1887, where it is associated with melinophanite, homilite, zircon, feldspar, molybdenite, cancrinite, and analcime (Palache *et al.* 1944). Subsequently, it was recognized in an ore pipe in marble near a granite contact at Arandis, Namibia (Ramdohr 1934), associated with tourmaline, cassiterite, calcite, siderite, stannite, chalcopyrite and pyrrhotite. Occurrences of nordenskiöldine in the Uchkoslkon tin deposit, eastern Kirgizia, and in Brukelin, Alaska, were reported by Marshukova *et al.* (1968) and Burt (1978), respectively. More recently, nordenskiöldine has been found in the Gejiu tin deposit, Yunnan (Wei *et al.* 1982), in the Dading tin–iron deposit (Wang 1983), and in a fluorite deposit in Jiangsu (Chen *et al.* 1987), in the People's Republic of China.

Nordenskiöldine, $CaSn(BO_3)_2$, was considered to be isostructural with dolomite, $CaMg(CO_3)_2$ (Ehrenberg & Ramdohr 1935, Aléonard & Vicat 1966), a hypothesis confirmed by a recent refinement of the structure (Effenberger & Zemann 1986). The spectroscopy of nordenskiöldine has seldom been reported, except for a Mössbauer spectrum of ^{119}Sn (Smith & Zuckerman 1967), an infrared spectrum (Suknev & Diman 1969) and luminescence spectra (Gaft *et al.* 1981, 1982, Gorobets 1988), partly because of its scarcity. In this work, the experimental infrared and Raman spectra of nordenskiöldine are presented. Bands are assigned by a calculation of normal modes and by a comparison with the results for the isostructural dolomite. We propose a possible mechanism for the splitting of the internal vibrational modes of nordenskiöldine, and discuss differences in the spectral properties and bonding of dolomite and nordenskiöldine.

Experimental Methods

The nordenskiöldine sample studied in this work was collected from the Gejiu tin deposit, Yunnan, China. There, the nordenskiöldine occurs in an andradite – diopside skarn belt in a normal contact zone between granite and carbonate host-rock. This skarn belt itself constitutes a new type of tin ore deposit in which the main Sn-bearing ore minerals are nordenskiöldine [$CaSn(BO_3)$], schoenfliesite [$MgSn(OH)_6$] and varlamoffite [$(Sn,Fe)(O,OH)_2$]. Cassiterite is seldom encountered. The nordenskiöldine occurs as colorless and transparent euhedral crystals with prominent {0001} cleavage. The crystals are thin or thick hexagonal tabular parallel to (0001). It is commonly replaced by schoenfliesite. Electron-microprobe and wet-chemical analyses are combined to determine the chemical compositions of the nordenskiöldine. The electron-microprobe analysis was performed at a voltage of 20 kV, a current of 0.06 μA, by point-to-point scanning on the nordenskiöldine sample. The average composition obtained is 53.67% SnO_2, 19.83% CaO, 0.26% MgO, 0.15% (total iron) FeO, and 0.08% MnO. The content of B_2O_3 in this sample was determined by the wet-chemical analysis to be 25.34%. The calculated chemical formula of the nordenskiöldine is: $(Ca_{0.979}Mg_{0.018}Fe_{0.006}Mn_{0.003})_{\Sigma 1.006}Sn_{0.986}(B_{1.008}O_3)_2$.

The X-ray-diffraction pattern was measured using Cu$K\alpha$ radiation and Ni filter and 114.57 mm diameter Debye–Scherrer camera. The unit-cell parameters of this sample, as derived by least-squares refinement of the powder data, are: a 4.857(1), c 16.035(6) Å, V 327.6(2) Å^3.

The infrared spectrum of this sample of nordenskiöldine was measured using a PE–580B spectrophotometer in the absorption mode from 200 to 2000 cm^{-1}. The sample was prepared as KBr pellets with a sample concentration of 2% by weight. The Raman spectrum was collected using an OMARS–89 micro-Raman spectrometer in the multichannel mode in three ranges of energy (200–840, 840–1400 and 1400–1600 cm^{-1}). An argon ion laser beam, whose wavelength is 457.94 nm, was used as the excitation source, with 120 mW of power and an aperture of 200 μm at room temperature.

Calculation of Normal Modes

A calculation of normal modes was performed, based on the all-valence force-field model, to obtain the theoretical frequencies, intensities and atomic displacements for vibrations observable in infrared and Raman spectra for nordenskiöldine and dolomite. Input information required by this calculation includes the unit-cell parameters and the space group of a crystal, the atomic masses, and the locations of one atom for each equivalent set, and a set of force constants that include conventional two-atom bonds, three-atom angles and interactions of internal coordinates that share at least one atom (Dowty 1987). The essential procedures of this calculation are as follows: (1) locate all atoms in the unit cell and compute displacement vectors for each internal coordinate, (2) convert the basis of the force constants from bonds and angles to cartesian displacements, (3) construct the full-matrix irreducible representations of the factor group, using appropriate symmetry matrices and polynomial basis-functions, (4) derive the symmetry coordinates in terms of cartesian displacement, using the projection-transfer operator techniques, (5) construct secular equations for each species with the Wilson F–G method (Shimanouchi *et al.* 1961), (6) solve frequencies for atomic motions, (7) use simple models of infrared and Raman intensity to calculate spectra, and (8) adjust the force constants by an iterative least-square technique to fit the experimentally observed spectra.

Results and Discussion

For an isolated planar ion group XO_3 (*e.g.*, BO_3^{3-} and CO_3^{2-}) having trigonal symmetry, there are four fundamental vibration modes, the symmetric stretching mode ν_1, the out-of-plane bending mode ν_2, the doubly degenerate asymmetric stretching mode ν_3, and the doubly degenerate planar bending mode ν_4. Of these vibrational modes, the ν_2, ν_3 and ν_4 modes are infrared-active, whereas the ν_1, ν_3 and ν_4 modes are Raman-active. In a crystalline solid containing such an anionic group as XO_3, the selection rules for vibrations are relaxed compared to vibrations for the isolated anionic groups, and the interaction between the modes may even remove degeneracies. In this case, the factor-group and site-group correlation analysis can reasonably explain the infrared and Raman spectra of the solids, for example, calcite and aragonite. For the dolomite structure, the correlation analysis of the factor group and site groups shows:

$$\Gamma_{vib} = 4A_g^{(R)} + 4E_g^{(R)} + 5A_u^{(IR)} + 5E_u^{(IR)}$$

in which there are four infrared-active internal modes $2A_u$ and $2E_u$, and four Raman-active internal modes $2A_g$ and $2E_g$. Therefore, the infrared-inactive symmetric stretching mode ν_1 and Raman-inactive out-of-plane bending mode ν_2 in the isolated ion XO_3 are activated symmetrically in the vibrational spectra of the dolomite structure.

The experimental infrared and Raman spectra of nordenskiöldine are shown in Figure 1 and 2, respectively, along with the corresponding infrared and Raman spectra of dolomite. The vibrational spectra of nordenskiöldine are predicted by the factor-group and site-group correlation mentioned above. All four infrared-active internal modes $2A_u$ and $2E_u$, and four Raman-active internal modes $2A_g$ and $2E_g$, are observed experimentally. Furthermore, normal mode calculations are carried out for nordenskiöldine and dolomite. The experimental and calculated results on the infrared and Raman spectra of nordenskiöldine and dolomite are summarized in Table 1. For dolomite, the calculated and measured frequencies for the lattice modes have larger deviations, and the Raman-active lattice mode E_g at 461 cm^{-1} is not observed experimentally. However, the calculated frequencies, intensities and symmetric assignments for the rest of

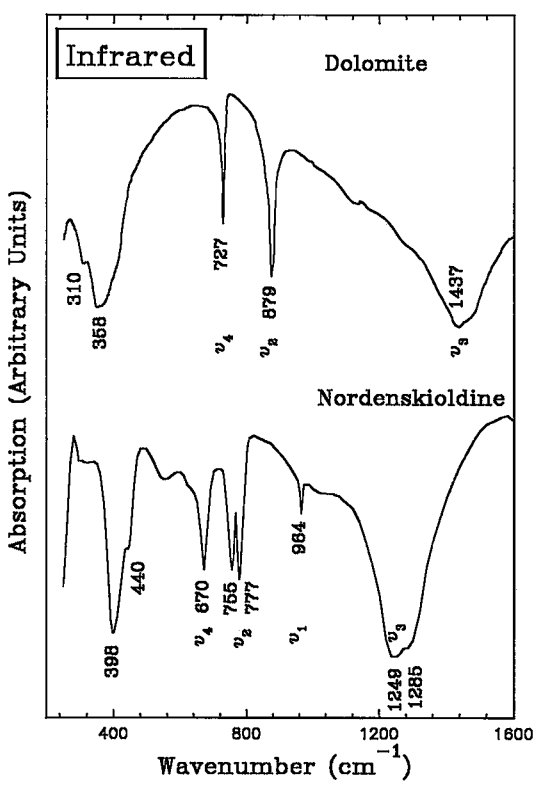

FIG. 1. Infrared-absorption spectrum of nordenskiöldine, $[CaSn(BO_3)_2]$, along with the infrared spectrum of the isostructural dolomite (Farmer 1974).

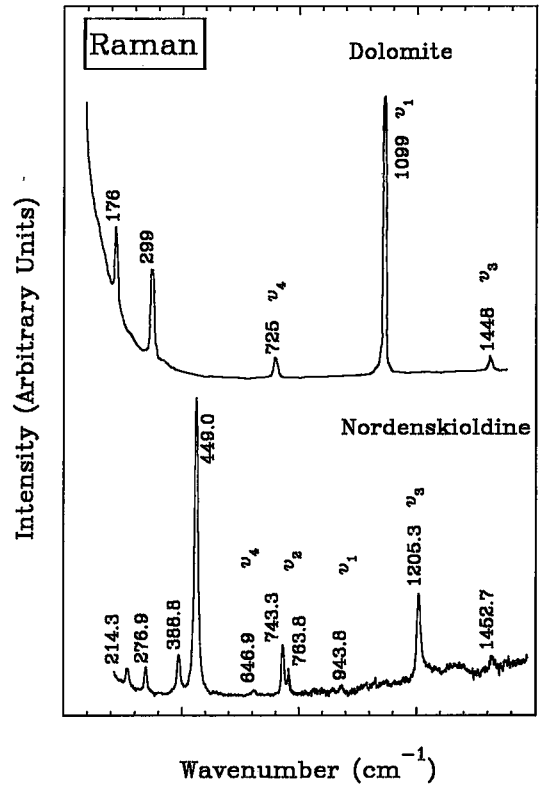

FIG. 2. Raman spectrum of nordenskiöldine, $[CaSn(BO_3)_2]$, along with the Raman spectrum of the isostructural dolomite (Farmer 1974).

TABLE 1. INFRARED AND RAMAN SPECTRA AND ASSIGNMENTS OF NORDENSKIÖLDINE AND DOLOMITE

			Nordenskiöldine				
Vibrational modes			Infrared			Raman	
			Meas.	Calc.		Meas.	Calc.
Internal modes	υ_1	A_u	964.0	927.8	A_g	943.8	927.0
	υ_2	A_u	777.0	762.1	A_g	763.8	750.0
			755.0	685.9		743.8	668.9
	υ_3	E_u	1285.0	1288.1	E_g		1279.8
			1249.0	1254.8		1205.3	1246.8
	υ_4	E_u	670.0	660.1	E_g	646.9	668.9
Lattice modes		A_u	440.0	435.2	A_g	449.0	457.5
		E_u	396.0	380.6	E_g	388.8	407.2
		A_u		218.5	E_g	276.9	222.9
		E_u		213.0	A_g	214.8	178.5
		A_u		159.5			
		E_u		135.3			
overtone $\upsilon_1+\upsilon_4$ or $2\upsilon_2$						1452.7	

			Dolomite				
Vibrational modes			Infrared			Raman	
			Meas.	Calc.		Meas.	Calc.
Internal modes	υ_1	A_u		1095.9	A_g	1099.0	1094.7
	υ_2	A_u	879.0	862.2	A_g		846.6
	υ_3	E_u	1437.0	1438.7	E_g	1448.0	1431.7
	υ_4	E_u	727.0	736.0	E_g	725.0	706.0
Lattice modes		A_u	362.0	397.0	E_g		461.1
		E_u	327.0	286.1	A_g	335.0	373.4
		A_u	314.0	265.5	E_g	299.0	245.7
		E_u	263.0	245.7	A_g	176.0	146.0
		E_u	157.0	205.7			
		A_u	162.0	95.4			

TABLE 2. FORCE CONSTANTS OF BO_3^{3-} GROUP IN NORDENSKIÖLDINE AND CO_3^{3-} GROUP IN DOLOMITE

Nordenskiöldine		Dolomite	
Bonds (md/Å)			
Ca-O	0.50	Ca-O	0.718
Sn-O	0.60	Mg-O	0.688
B-O	4.00	C-O	5.620
O-O	0.90	O-O	1.272
Angles (md-Å/rad)			
O-B-O	0.68	O-C-O	0.858
Interaction (md/Å)			
B-O/B-O	0.51	C-O/C-O	0.566

modes, especially for the internal modes of CO_3^{2-} group, are in a good agreement with experimental infrared and Raman spectra of dolomite (Farmer 1974). The infrared-active ν_1 band and Raman-active ν_2 band are so weak that they are not observed experimentally. This comparison indicates that the normal mode calculation is useful for the reliable assignment of vibrational modes.

For nordenskiöldine, the experimental spectra are reasonably assigned to the corresponding vibrational modes as shown in Table 1, based on the normal mode calculation for nordenskiöldine and a comparison with dolomite. The infrared and Raman spectra for nordenskiöldine are characterized by its internal modes. The peaks below 450 cm^{-1} are attributed to the lattice modes, but some of these lattice modes are not measured in the infrared spectrum of the powder sample. The lattice mode at 449 cm^{-1} seems too strong in the Raman spectrum to be correctly assigned. In addition, the weak Raman peak at 1452.7 cm^{-1} is assigned to the overtone modes $\nu_1 + \nu_4$, or $2\nu_2$ (Hutt & Ninola 1974).

Figure 1 and Table 1 indicate that the infrared-absorption spectrum for nordenskiöldine differs from those of calcite-structure $LuBO_3$, aragonite-structure $NdBO_3$, vaterite-structure YBO_3 (Weir & Lippincott 1961); the infrared and Raman spectra for nordenskiöldine also are different from those of the isostructural dolomite. It is apparent that in both infrared and Raman spectra of nordenskiöldine, the lattice vibrational modes shift to higher energy compared to those for dolomite. In contrast, the internal modes of the BO_3^{3-} group in nordenskiöldine shift toward the lower frequencies in comparison to the corresponding internal modes of the CO_3^{2-} group in dolomite. The results are consistent qualitatively with apparent differences in bond lengths and force constants of the B–O bond in nordenskiöldine and of the C–O bond in dolomite (Table 2). Such differences in vibrational behavior of the B–O and C–O bonds are related to the crystal-chemical properties and bonding of boron and carbon. Carbon has a smaller ionic radius and is more strongly electronegative than boron. Hence the C–O bonds in dolomite are more covalent and have shorter bond-lengths than the B–O bonds in nordenskiöldine. In addition, the bonding of cations with oxygen in nordenskiöldine is stronger than that in dolomite. As a result, the internal modes in the infrared and Raman spectra of dolomite are more similar to those of the free group CO_3^{2-}, the internal modes of BO_3^{3-} in nordenskiöldine shift to lower energy, and the lattice modes shift to high energy, relative to the corresponding modes for dolomite.

Lattice vibrations in both infrared and Raman spectra of nordenskiöldine are strong. In particular, the strong Raman scattering peak at 449 cm^{-1} is unexpected. Regarding the internal modes, the symmetric stretching mode ν_1 for dolomite is the strongest Raman peak, but it is not observed in the infrared-absorption spectrum. However, for nordenskiöldine, the ν_1 becomes apparently observable in the infrared spectrum, and weak in the Raman spectrum. The out-of-plane bending mode ν_2, which is strong in the infrared spectrum, but very weak in the Raman spectrum for dolomite, is observed as two strong peaks in both infrared and Raman spectra of nordenskiöldine. The asymmetrical stretching mode ν_3 becomes much stronger in both infrared and Raman spectrum of

nordenskiöldine, but is split and asymmetrical in the infrared spectrum. The in-plane bending mode ν_4 seems similar for both nordenskiöldine and dolomite. On the other hand, the calculation of normal modes indicates that the Raman-active internal modes for nordenskiöldine have greater intensity than the corresponding modes for dolomite. This is in agreement with the electric dipole polarizabilities of borate and carbonate calculated using the first-principles quantum-mechanical method. Tossell (1990) showed that the average polarizabilities are 4.21 for BO_3^{3-} and 3.41 for CO_3^{2-}. On the other hand, the calculated average polarizability and polarization anisotropy for BO_3^{3-} and CO_3^{2-} are qualitatively related to relative energies of the a_1', a_2'' and e' symmetry unoccupied molecular orbitals of the oxyanions. For example, the larger change in $\alpha_\parallel$ for BO_3^{3-} and CO_3^{2-} comes from the $1a_2''$ contribution, which is much larger for BO_3^{3-} owing to the much smaller $1a_2'' \rightarrow 5a_1'$ energy difference. Therefore, the difference in relative intensities for the Raman internal modes of nordenskiöldine and dolomite is indeed related to differences in the electronic structure and bonding.

Another difference between nordenskiöldine and dolomite lies in the splitting of ν_2 and ν_3 modes in both infrared and Raman spectra of nordenskiöldine. This is not predicted by the factor-group and site-group correlation analysis. Actually the splitting of ν_2 and ν_3 modes has also been observed in the infrared spectra of many other orthoborates, for example, $PrBO_3$ (Laperches & Tarte 1966), $LaBO_3$ (Steele & Decius 1956), and $Mg_3(BO_3)_2$, $Ca_3(BO_3)_2$ and $Cd_3(BO_3)_2$ (Mitchell 1966). The splitting of the doubly degenerate ν_3 and ν_4 in the infrared spectra of solids containing the XO_3 ions is generally due to the lower site-group symmetry of X ions than C_3, as in aragonite. However, this interpretation is not plausible for nordenskiöldine. First, the crystallographic data indicate that the site group of BO_3 group in nordenskiöldine is C_3 (Effenberger & Zemann 1986); hence, the splitting of the doubly degenerate ν_3 and ν_4 caused by the site group is unexpected. Second, in our measured infrared and Raman spectra, the splitting of the ν_4 mode actually was not observed, whereas the nondegenerate out-of-plane bending mode ν_2 was measured as two split peaks. In addition, the coupling mechanism between internal modes was proposed to explain the characteristic infrared spectra of borates. However, our calculation of normal modes for nordenskiöldine showed little or no variation of the ν_2 and ν_3 modes with the coupling interaction, which, in fact, is similar for both dolomite and nordenskiöldine. Therefore, the splitting of each of the ν_2 and ν_3 modes into two peaks in the infrared and Raman spectra of nordenskiöldine is probably due to the substitution effect involving both B^{10} and B^{11}. First, because the natural abundances of the two stable isotopes of boron, B^{11} and B^{10}, are 80.22% and 19.78%, respectively, the coexistence B^{11} and B^{10} in natural borate minerals, such as nordenskiöldine, is not surprising. Second, for $LaBO_3$, $InBO_3$ and $ScBO_3$ (Steele & Decius 1956), and $Mg_3(BO_3)_2$, $Ca_3(BO_3)_2$, $Sr_3(BO_3)_2$ and $Ba_3(BO_3)_2$ (Weir & Schroeder 1964), when B^{10} substitutes for B^{11}, the ν_1 and ν_4 modes in the infrared absorption spectra do not show observable shifts; however, significant shifts for the ν_2 and ν_3 modes were observed. Our experimental results are in good agreement with these observations. Third, in the infrared-absorption spectrum of $LaBO_3$, the frequency differences for the ν_2 and ν_3 modes due to the substitution of B^{10} for B^{11} are about 28 and 44 cm^{-1}, respectively (Steele & Decius 1956). The frequency differences for the ν_2 and ν_3 modes in the infrared spectrum of nordenskiöldine are 22 and 36 cm^{-1}, respectively, also in good agreement with the results for $LaBO_3$. Therefore, the splitting of the ν_2 and ν_3 modes in both infrared and Raman spectra of nordenskiöldine is attributed to the substitution of B^{10} for B^{11}.

Conclusions

Bands in the infrared and Raman spectra of nordenskiöldine, a rare orthoborate, are assigned to the corresponding vibrational modes by the calculation of normal modes with an all-valence force-field model and by a comparison with the results for the isostructural dolomite. The shifts for the internal modes to lower energy and the shifts to higher energy in nordenskiöldine, relative to those of dolomite, are due to the weak covalency of B–O bonds and stronger cation–oxygen bonding. The larger Raman intensity calculated for nordenskiöldine is related to the larger electric dipole polarizability of BO_3^{3-}, which is further related to the much smaller $1a_2'' \rightarrow 5a_1'$ energy difference, as calculated by the first principles quantum-mechanical method. The characteristic double peaks for the out-of-plane bending mode ν_2 and the symmetric stretching mode ν_3 of BO_3^{3-} ion in nordenskiöldine are attributed to the isotopic substitution effect of B^{11} and B^{10}.

Acknowledgements

The authors appreciate the assistance provided by Mary Jean Walzak at Surface Science Western, London, Ontario, and Yuansheng Lou at Beijing Institute of Geology and Mineral Resources, for the measurements of Raman and infrared spectra, respectively. This work was partly supported by the National Science Foundation of China. We thank E. Dowty for his program, used in our calculations, and G. Henderson, for allowing us to use the program. We thank Professors R.F. Martin, G. Calas, J. Zemann and an anonymous referee for their comments and suggestions, which led to significant improvements in this paper.

REFERENCES

ALÉONARD, S. & VICAT, J. (1966): Borates de structure dolomies. *Bull. Soc. Franç. Minéral. Cristallogr.* **89**, 217-272.

BURT, D.M. (1978): Tin silicate – borate – oxide equilibria in skarns and greisens – the system $CaO–SnO_2–SiO_2–H_2O–B_2O_3–CO_2–F_2O_{-1}$. *Econ. Geol.* **73**, 269-282.

CHEN SISONG, WEI JINGSHENG & HUANG KEBING (1987): Discovery of nordenskiöldine in Jiangsu Province. *Yanshi Kuangwuxue Zazhi* **6**, 364-367 (in Chinese).

CHRIST, C.L. (1960): Crystal chemistry and systematic classification of hydrated borate minerals. *Am. Mineral.* **45**, 334-340.

DOWTY, E. (1987): Fully automated microcomputer calculation of vibrational spectra. *Phys. Chem. Mineral.* **14**, 67-79.

EDWARDS, J.O. & ROSS, V. (1960): Structural principles of the hydrated polyborates. *J. Inorg. Nucl. Chem.* **15**, 329-337.

EFFENBERGER, H. & ZEMANN, J. (1986): The detailed crystal structure of nordenskiöldine, $CaSn(BO_3)_2$. *Neues Jahrb. Mineral., Monash.*, 111-114.

EHRENBERG, H. & RAMDOHR, P. (1935): Die Struktur des Nordenskiöldine. *Neues Jahrb. Mineral. Geol. Palaeontol., Abh.* **69**, *Abt.* **A**, 1-4.

FARMER, V.C. (1974): *The Infrared Spectra of Minerals.* The Mineralogical Society, Monogr. **4**.

GAFT, M.L., GOROBETS, B.S. & MALINKO, S.V. (1981): Possibilities for the use of luminescence for rapid detection and identification of boron minerals in rock. *Nov. Dannye. Mineral. SSSR* **29**, 36-43 (in Russ.).

———, ———, MARSHUKOVA, N.K. & PAVLOVSKIY, A.B. (1982): Luminescence of tin minerals and its use in the study of tin ore deposits. *Dokl. Acad. Sci. USSR, Earth Sci. Sect.* **266**, 113-115.

GOROBETS, B.S. (1988): X-ray luminescence spectra of minerals and ore-forming criteria for ore beneficiation. *Mineral. Sb.* **42**, 74-80 (in Russ.).

HUTT, H.N. & NINOLA, J.H. (1974): Raman spectra of carbonates of calcite structure. *J. Phys. C: Solid State Phys.* **7**, 4522-4528.

LAPERCHES, J.P. & TARTE, P. (1966): Spectres d'absorption infrarouge de borates de terres rares. *Spectrochim. Acta* **22**, 1201-1210.

MARSHUKOVA, N.K., SIRINA, T.N. & PAVLOVSKIY, A.B. (1968): First find of nordenskiöldine in the U.S.S.R.. *Zap. Vses. Mineral. Obshchest.* **97**, 695-698 (in Russ.).

MITCHELL, A. (1966): Infra-red absorption of the orthoborate ion. *Trans. Faraday Soc.* **62**, 530-533.

PALACHE, C., BERMAN, H. & FRONDEL, C. (1944): *Dana's System of Mineralogy* **2**. John Wiley & Sons Inc., New York.

RAMDOHR, P. (1934): Nordenskiöldine in einer Zinnerzlagerstätte. *Neues Jahrb. Mineral. Geol. Palaeontol., Abh.* **68**, *Abt.* **A**, 288-295.

SHIMANOUCHI, T., TSUBOI, M. & MIYAZAWA, T. (1961): Optically active lattice vibrations as treated by the GF-matrix method. *J. Chem. Phys.* **35**, 1597-1612.

SMITH, D.L. & ZUCKERMAN, J.J. (1967): ^{119}Sn Mössbauer spectra of tin-containing minerals. *J. Inorg. Nucl. Chem.* **29**, 1203-1210.

STEELE, W.C. & DECIUS, J.C. (1956): Infrared absorption of lanthanum, scandium, and indium borate and the force constants of borate ion. *J. Chem. Phys.* **25**, 1184-1188.

SUKNEV, V.S. & DIMAN, E.N. (1969): The infrared spectra of nordenskiöldine and its analogs. *Zh. Prikl. Spectrosk.* **10**, 326-331 (in Russ.).

TOSSELL, J.A. (1990): First principles quantum mechanical calculation of the electric dipole polarizabilities of the borate, carbonate, nitrate and related ions. *Phys. Chem. Minerals* **17**, 133-141.

WANG SHUFENG (1983): geochemistry of the Dading tin-iron ore deposits. *Zhongguo Dizhi Kexueyuan Kuangchan Dizhi Yanjiuso Sokan* **9**, 72-84 (in Chinese).

WEI MINGXIU, WANG FENGGE & YIN CHENGYU (1982): Nordenskiöldine discovered in China and its formation conditions. *Acta Mineral.* **4**, 262-266 (in Chinese).

WEIR, C.E. & LIPPINCOTT, E.R. (1961): Infrared studies of aragonite, calcite, and vaterite type structures in the borates, carbonates, and nitrates. *J. Res. Nat. Bur. Stand.* **65A**, 173-183.

——— & SCHROEDER, R.A. (1964): Infrared spectra of the crystalline inorganic borates. *J. Res. Nat. Bur. Stand.* **68A**, 465-487.

WELLS, A.F. (1984): *Structural Inorganic Chemistry* (5th ed.). Oxford University Press, Oxford, U.K.

Received January 22, 1993, revised manuscript accepted June 23, 1993.